20th Australasian Fluid Mechanics Conference
Perth, Australia
5-8 December 2016

Time Resolved Measurements of Wake Characteristics from Vertical Surface-Piercing Circular Cylinders

S. J. Keough[1,2], I. L. Kermonde[1], A. Amiet[1], J. Philip[2], A. Ooi[2], J. P. Monty[2] and B. Anderson[1]

[1]Maritime Division
Defence Science and Technology Group, Fishermans Bend, Victoria 3207, Australia

[2]Department of Mechanical Engineering
University of Melbourne, Parkville, Victoria 3010, Australia

Abstract

Towing tank experiments were conducted at the Australian Maritime College facility in Launceston, measuring the size and shape of the wake generated by two different diameter cylinders pulled through the free surface at a range of speeds. Measurements of the bow wave run up height have been compared with previous experimental data and have been shown to be consistent with these results. For low Froude numbers, the maximum bow wave height scales with velocity as predicted by Bernoulli's equation for inviscid flow. As velocity increases, the deviation from the inviscid flow prediction increases accordingly and can be modelled by adding a dissipation term to Bernoulli's equation.

Previous studies have presented measurements of the wake as mean or single snapshot values of the flow characteristics. With increasing Froude number, the height of the bow wave oscillates around the mean value such that time resolved measurements are required to properly capture the flow behaviour. In this work, video analysis of the wake has been used to observe the variation in this characteristic measurement, allowing accurate calculation of the mean and standard deviation, as well as investigation into the frequency of the oscillations.

Introduction

A common method for experimentally determining the size and shape of wake from a cylinder moving through a free surface is to conduct a towing tank experiment. Hay [3] presents the most comprehensive collection of such experiments and provides a template of measurements by which the size and shape of the wake can be characterised. The bow wave height (D_1) shown in Figure 1, is one such measurement and is the focus of the present study. Other investigations [1, 2] have been carried out similar to this work, while focusing on relatively large diameter cylinders penetrating the free surface to greater depths, so as to eliminate end effects. Chaplin and Teigen [1] describe the theoretical maximum bow wave height by rearranging Bernoulli's equation for inviscid flow ($V^2/2 = gD_1$) such that the non-dimensional height (D_1/d) depends on the Froude number based on the diameter ($Fr_d = V^2/\sqrt{gd}$, where V is the velocity and d is the diameter of the cylinder), suggesting that this equation is expected to hold true for a circular cylinder at high Reynolds numbers and low Froude numbers.

$$\frac{D_1}{d} = \frac{Fr_d^2}{2} \tag{1}$$

Each of the previous works present measurements of the bow wave run up height, mostly measured at a single point in time. At low Froude numbers, the flow in the bow wave is steady, so a single measurement provides an accurate description of the shape. However, as the Froude number increases, the flow in the bow wave becomes chaotic, causing the height of the bow wave to vary. As such, the D_1 value can no longer be measured by a snapshot approach without introducing an error term representing the variability. Using video capture to record the flow allows investigation of these unsteady variations and calculation of accurate mean and standard deviation values for the bow wave height measurement.

Figure 1: Measured maximum height of the bow wave (D_1). Here the cylinder is towed from right to left.

A feature of the wake behind cylinders pulled through a fluid is the Kármán vortex street; whereby a series of vortices are shed from alternating sides of the cylinder, at a frequency (f) dependent on the Strouhal number (St) [4].

$$f = St\frac{V}{d} \tag{2}$$

A Kármán vortex street is expected to occur with a Reynolds number in the range $300 < Re < 3\times10^5$. In this range, the Strouhal number is expected to be approximately constant at $St = 0.2$ [4]. For the experiments presented here the Reynolds numbers were in the range $4.5\times10^4 < Re < 3.8\times10^5$ (Table 1), with only two of the runs exceeding the expected threshold for generation of the vortex street. Vortex shedding produces a small variation in the drag force on the cylinder, at twice the vortex shedding frequency. This effect is likely to cause the pressure at the front of the cylinder to fluctuate at the same rate, potentially generating a cyclic variation in the bow wave height as predicted by Bernoulli's equation. Frequency analysis performed on the transient bow wave height will allow investigation into whether this relationship can be observed experimentally.

Methodology

Towing Tank Experiments

For these experiments, the towing tank located at the Australian Maritime College at the University of Tasmania has been used. This towing tank measures 100 m long by 3.55 m wide and was filled to a nominal water depth of 1.5 m. Cylinders of 100 mm and 216 mm diameter were mounted to the towing carriage such that the bottom of the cylinder reached 840 mm below the surface. The towing tank is capable of towing models up

Table 1: Froude and Reynolds numbers for experimental runs

Diameter (mm)	Velocity (m/s)	Fr_d	Re
100	0.5	0.505	45,656
	1.0	1.01	91,312
	1.5	1.515	136,968
	2.0	2.02	182,623
	2.5	2.525	228,279
	3.0	3.03	273,935
216	0.5	0.349	95,877
	1.0	0.697	191,755
	1.5	1.046	287,632
	1.75	1.22	335,570
	2.0	1.394	383,509

to 4.6 $\mathrm{m\,s^{-1}}$ however due to the large drag force produced, the experimental runs were limited to a maximum of 3 $\mathrm{m\,s^{-1}}$ and 2 $\mathrm{m\,s^{-1}}$ for the 100 mm and 216 mm cylinders respectively. The cylinders were coloured with alternating yellow and black horizontal stripes of 10 mm increment and wooden rulers were attached to the towing carriage to allow for scaled measurements to be extracted from recorded imagery. Cameras were placed in a range of locations attached to both the towing carriage and to the viewing window on the side of the towing tank and video was recorded at 120 fps. For analysis of the bow wave height, video taken from in front of the cylinder was used (Figure 2).

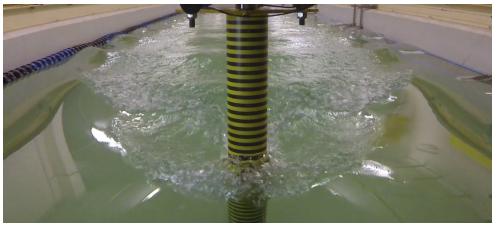

Figure 2: 100 mm cylinder as viewed from the front of the towing carriage

Video Processing

Using the yellow and black stripes on the cylinders as a calibration scale, the bow wave height at the front of the cylinder can be extracted from the video footage as a function of time by measuring the height in each frame. Doing these measurements manually is prohibitively time consuming so a method of automatically tracking the height of the bow wave was created. The software written to track the bow wave height takes each frame of the video and crops it to include only the cylinder. An image of the cylinder while stationary is used as a background and subtracted from the current frame. The result is converted to black and white such that only areas where the image has changed from the background show white. Spurious regions of white—created by changing lighting as the towing carriage moves and small movements in the camera position—are removed by dilating and filling then eroding the white regions, leaving a clear edge highlighting the top of the bow wave. A simple edge detection process is used to remove any remaining outliers and the instantaneous bow wave height is taken as the root mean square of the maximum height in each pixel column across the cropped image. Figure 3 shows the progression of the processed image using this method.

Figure 4 shows a small sample of one run, comparing the result of the automated bow wave height tracking with manual measurement of the same run. Comparison between the automatic and manually measured data for this run shows a strong

Figure 3: Progression of image processing used to isolate the bow wave for automated tracking. (a) cropped raw video; (b) background subtracted black and white; (c) dilated and filled; (d) final image used for tracking.

Pearson correlation of 0.839, highlighting that the automated process is able to accurately track the variations in time. The difference between measured values is seen to be less than the experimental error expected in the manual process ($\pm$5 mm), as seen in Table 2, which shows a comparison between the calculated characteristic values.

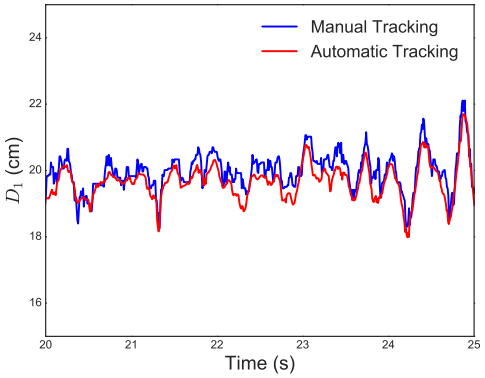

Figure 4: Sample of measured bow wave height (D_1) for the 216 mm cylinder at 2 $\mathrm{m\,s^{-1}}$, comparing automated and manual measurement.

Table 2: Calculated values comparing manual measurement with automated bow wave height tracking for the run shown in Figure 4

	Manual	Automatic
Mean D_1 (cm)	19.88	19.58
Standard Deviation D_1 (cm)	0.55	0.52
Pearson Correlation Coefficient	0.839	

Frequency Analysis

Frequency analysis was performed by calculating an estimate of the power spectral density (PSD) using the Welch method [8]. A Savitsky-Golay [6] filter was applied to the data to remove noise observed to be present at smaller and relatively larger scales. Note that the high frequency lobes in the PSD are a consequence of this filter, which was tolerable since we were mostly interested in relatively lower frequencies. Subsequently, the spectra were generated by implementing a Nuttall windowing function (minimum 4-term Blackman-Harris window [5]) on 5 second segments of signal with 50% overlap and averaging the discrete Fourier transform of each segment. In the cases where multiple runs had been completed with the same cylinder at the same speed, the PSD's for each run were then averaged to

further reduce noise.

Results

At very low Froude numbers ($Fr_d \leq 0.5$) the flow in the bow wave is steady, with very little variation in the run up height over time. As the Froude number increases, unsteady chaotic motion appears and increases in size until the bow wave begins to break, at which point the flow is dominated by the unsteady chaotic motion; Figure 5 highlights this transition. The breaking wave introduces a cyclic mechanism in which water is pushed forward and crashes in front of the cylinder before recirculating back into the bow wave and contributing to the unsteady variation in the run up height.

(a) $Fr_d = 0.505$ (b) $Fr_d = 1.01$ (c) $Fr_d = 1.515$

Figure 5: As Fr_d increases, the flow transitions from steady flow at $Fr_d \leq 0.5$ (a), through the appearance of some unsteady chaotic motion $0.5 \leq Fr_d \leq 1.5$ (b), to unsteady breaking waves $Fr_d \geq 1.5$ (c).

Figure 6 shows the measured height (D_1) for the 100 mm cylinder across a range of velocities from 0.5 $\mathrm{m\,s^{-1}}$ to 3 $\mathrm{m\,s^{-1}}$ (Fr_d from 0.505 to 3.03). It can be seen that as the velocity increases, both the mean height and the amplitude of transient variations increase.

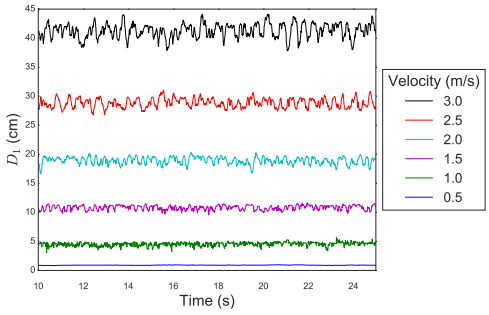

Figure 6: Time resolved D_1 measurement for the 100 mm cylinder at a range of speeds from 0.5 $\mathrm{m\,s^{-1}}$ to 3 $\mathrm{m\,s^{-1}}$

For the purpose of this experiment, we write Bernoulli's equation as:

$$D_1 = \frac{V^2}{2g} \tag{3}$$

This equation highlights the important point that the bow wave height is, in theory, independent of the diameter of the cylinder. Figure 7 shows the theoretical bow wave height plotted against our experimental results for both the 100 mm and 216 mm cylinders, as well as for data taken from previous experiments [1, 2], showing an identical near linear relationship between the mean D_1 and V^2 for each experimental dataset.

It can also be seen that at higher velocities (thus higher Froude number), the measured D_1 begins to fall away from the inviscid flow prediction due to increasing energy dissipation. For fully turbulent flow, energy dissipation is proportional to V^2 [7], so we model dissipation by $C_{dissp}V^2$, where C_{dissp} is a positive constant much smaller than $1/2g$. As such, we modify Bernoulli's equation to include the energy dissipation:

$$D_1 = \frac{V^2}{2g} - C_{dissp}\, V^2 \tag{4}$$

The dashed line in Figure 7 shows the predicted D_1 including the dissipation term with $C_{dissp} = 0.005$, and is observed to follow the experimental data reasonably well.

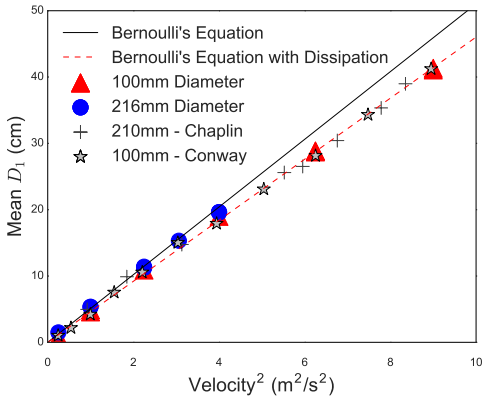

Figure 7: Mean D_1 values calculated from the present experiments, compared with results from previous works [1, 2]. The solid line shows the expected value, estimated using Bernoulli's equation for inviscid flow. The dashed line shows Bournoulli's equation including a dissipation term.

As the mean D_1 increases with velocity, the transient variation in D_1 increases approximately linearly as shown in Figure 8, which compares the standard deviation of each measurement to the mean. This linear variation is likely a consequence of the fact that a small variation in velocity (or more precisely V^2) due to any experimental uncertainty or other unknown physical phenomenon, is directly translated to a variation in the height as per Bernoulli's equation.

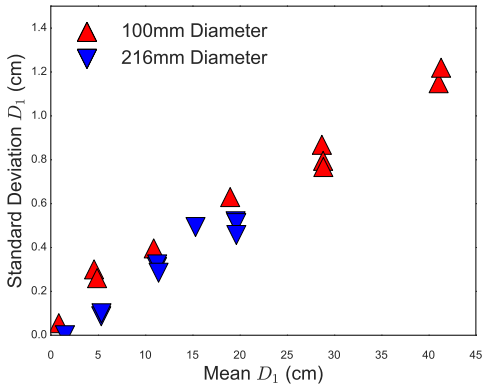

Figure 8: Standard deviation of D_1 against the mean

The power spectral density was calculated for runs at $Fr_d > 1.5$. For Froude numbers below $Fr_d = 1.5$, the flow in the bow wave is predominantly steady, with variation in the height generally less than the experimental error in the measurements. The results of the frequency analysis are shown as a stack plot in Figure 9. Each result exhibits a broad frequency peak in the region of 1-10 Hz however no clear single frequency peaks are observed, suggesting that any frequency effect expected due to

vortex shedding is likely to be too small to be easily distinguished from other effects in the signal.

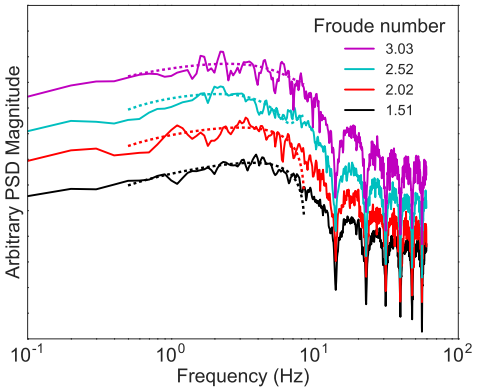

Figure 9: Stack plot of estimated power spectral density (PSD) for runs with $Fr_d > 1.5$. Dashed lines show the polynomial fit of the broad peak between 1-10 Hz.

As the Froude number increases, the broad peak in the spectrum appears to shift slightly towards lower frequencies. If we assume that for the inviscid flow prediction, the kinetic energy of the flow is entirely conserved and translated into potential energy at the peak of the bow wave, then the time taken for water in the breaking wave fall to back to the free surface level, accelerated only by gravity, would be given by V/g. If we then assume, for the perfectly conservative model problem, that the time taken to rise to the peak is also given by V/g, the cycle period for a crashing wave will be given by $2V/g$. Inverting this to extract a theoretical frequency for the cyclic wave crashing gives $f = 0.5g/V$, which would produce a peak shift toward lower frequencies with increasing velocity. In a non-conservative case, it may be possible to model the frequency as $f = C_{freq}g/V$, where C_{freq} is some constant less than 0.5, dependent on the energy dissipation. By applying a simple polynomial fit to the broad peak part of the spectra (shown as the dashed lines in Figure 9), we can approximate the peak value and plot it against g/V to determine if such a relationship exists. Figure 10 shows this data along with a linearly fitted line ($f = 0.46g/V + 0.64$). While this appears to show that a relationship of $f \propto g/V$ could exist, the small amount of data and the noise level in the frequency analysis make it difficult to come to any firm conclusions in this regard. In order to improve the confidence in this result, more data at the same Froude numbers is required to reduce the noise in the signal. Further data at higher Froude numbers would also enable better investigation of the relationship between the frequency and the Froude number.

Conclusions

Video analysis was used to investigate the transient nature of bow wave run up height measurements during towing tank experiments of cylinders being pulled through the free surface. It was observed that for Froude numbers below $Fr_d = 0.5$ the flow in the bow wave was steady, with unsteady chaotic flow appearing and increasing in size up to approximately $Fr_d = 1.5$ at which point the bow wave began to break and the flow became dominated by unsteady flow. A simple bow wave tracking algorithm was created and found to be as accurate as manual tracking methods to within the experimental error, allowing for accurate high frequency measurements of a large number of experimental runs. The time resolved data was used to calculate accurate mean bow wave height values, which were compared with results from previous experiments and shown to be

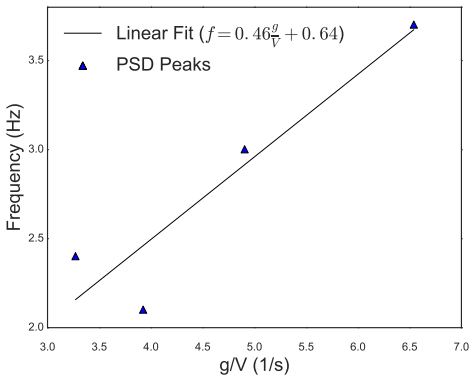

Figure 10: Plot of estimated power spectral density peaks against g/V with a linear fitted line

consistent. The measurements confirmed that for low Froude numbers, the bow wave height can be predicted by Bernoulli's equation for inviscid flow, which is independent of the size of the cylinder. As velocity increases, the deviation from the inviscid flow prediction can be modelled by including a dissipation term in Bernoulli's equation with a constant of dissipation approximately given by $C_{dissp} = 0.005$. Frequency analysis of the data showed that while effects due to vortex shedding from the cylinder could not be detected experimentally in the height of the bow wave, a cyclic effect from the breaking wave does occur that interacts with the height variation and is likely to affect the frequency according to some relationship $f \propto g/V$.

Acknowledgements

The authors would like to thank the staff at AMC for their assistance in preparing and operating the towing tank facility.

References

[1] Chaplin, J. and Teigen, P., Steady flow past a vertical surface-piercing circular cylinder, *Journal of Fluids and Structures*, **18**, 2003, 271–285.

[2] Conway, A., Binns, J., Ranmuthugala, D. and Renilson, M., Experimental and numerical analysis of submarine mast surface wakes, in *Pacific International Maritime Conference*, 2015, 1–12.

[3] Hay, A. D., *Flow about semi-submerged cylinders of finite length*, Princeton University, 1947.

[4] Lienhard, J. H., *Synopsis of lift, drag, and vortex frequency data for rigid circular cylinders*, Technical Extension Service, Washington State University, 1966.

[5] Nuttall, A., Some windows with very good sidelobe behavior, *IEEE Transactions on Acoustics, Speech, and Signal Processing*, **29**, 1981, 84–91.

[6] Savitzky, A. and Golay, M. J. E., Smoothing and differentiation of data by simplified least squares procedures., *Analytical Chemistry*, **36**, 1964, 1627–1639.

[7] Tritton, D. J., *Physical fluid dynamics*, Springer Science & Business Media, 2012.

[8] Welch, P., The use of fast fourier transform for the estimation of power spectra: A method based on time averaging over short, modified periodograms, *IEEE Transactions on Audio and Electroacoustics*, **15**, 1967, 70–73.